Hydrobiologia (2011) 661:235–250
DOI 10.1007/s10750-010-0528-9

PRIMARY RESEARCH PAPER

Temporal and spatial variability of chlorophyll *a* concentration in Lake Taihu using MODIS time-series data

Yuchao Zhang · Shan Lin · Xin Qian · Qin'geng Wang · Yu Qian · Jianping Liu · Yi Ge

Received: 24 May 2009 / Revised: 20 September 2010 / Accepted: 13 October 2010 / Published online: 26 October 2010

Abstract In order to predict the distribution of chlorophyll *a* synoptically in Lake Taihu from 2006 to 2008, a common empirical algorithm was developed to relate time series chlorophyll *a* concentrations in the lake to reflectance derived as a function of band 2 MODIS data ($r^2 = 0.907$, $n = 145$) using time series from 2005. The empirical model was further validated with chlorophyll *a* data from a 2008 to 2009 dataset, with RMSE < 7.48 μg l^{-1} and $r^2 = 0.978$. The seasonal and inter-annual variability of the surface chlorophyll *a* concentration from 2006 to 2008 was then examined using Empirical Orthogonal Function (EOF) analysis. The results revealed that the first four modes were significant, explaining 54.0% of the total chlorophyll *a* variance, and indicated that during the summer, algal blooms always occur in the northern bays, Meiliang Bay and Gonghu Bay, while they occur along the southwestern lakeshore during early summer, fall, and even early winter. The inter-annual variance analysis showed that the duration of algal blooms was from April to December of 2007, which was different from the bloom periods in 2006 and 2008. The results of EOF analysis show its potential for long-term integrated lake monitoring, not only in Lake Taihu but also in other large lakes threatened by accelerating eutrophication.

Keywords Algal blooms · Chlorophyll *a* · Empirical algorithms · EOF analysis

Handling editor: D. Hamilton

Y. Zhang · S. Lin · X. Qian (✉) · Q. Wang · Y. Qian · J. Liu · Y. Ge
State Key Laboratory of Pollution Control and Resource Reuse, School of the Environment, Nanjing University, Nanjing 210093, People's Republic of China
e-mail: xqian@nju.edu.cn

Introduction

Lake Taihu, third largest freshwater lake in China, is situated in the Yangtze River Delta (Fig. 1). Due to side-effects of economic and social development, algal blooms have frequently occurred in Lake Taihu since the 1980s (Hu et al., 2006). In 2007, algal blooms occurred 1 month earlier than in previous years, causing drinking water sources to be severely polluted and millions of people to be exposed to health hazards, which in turn imperiled the social stability of the region (Yang et al., 2008).

Currently, quantitative understanding of the temporal and spatial variability of chlorophyll *a* concentration in Lake Taihu is far from adequate. Accordingly, a better understanding could help scientific researchers, environmental managers and policy designers to know when, where, and why algal blooms occur in Lake Taihu. In order to accomplish a better understanding, remote sensing techniques can be used to supplement on-ground observations and laboratory experiments.

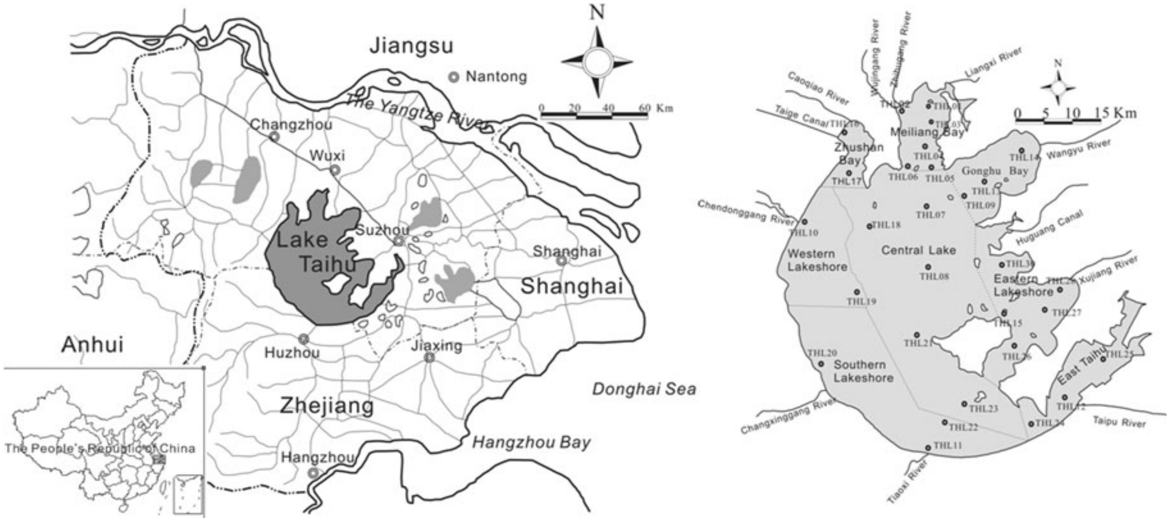

Fig. 1 Location map of Lake Taihu in the Yangtze River Delta of China. Annotated numbers show stations used to sample monthly during 2005 by the Taihu Ecosystem Research and Field Observation Station of the Chinese Academy of Sciences. The water body of Lake Taihu is divided into eight water regions: Meiliang Bay, Zhushan Bay, Gonghu Bay, Central Lake, Western Lakeshore, Southern Lakeshore, East Taihu and Eastern Lakeshore

During evaluation of water color by remote sensing, two types of waters, Case 1 and Case 2, have been distinguished (Yentsch, 1984). Inland waters such as Lake Taihu belong to Case 2 waters, which are influenced by phytoplankton and associated organic matter, as well as other substances that vary independently of phytoplankton, such as inorganic particles in suspension and chromophoric dissolved organic matter (CDOM). It is well known that the standard algorithms in use for chlorophyll *a* retrieval from Case 1 waters break down in Case 2 waters (IOCCG, 2000; Dall'Olmo et al., 2005). Accordingly, many studies have been conducted to evaluate methods to derive chlorophyll *a* in different turbid waters using bio-optical models. All of these models are based on the spectral properties near 700 nm rather than in the blue (c. 440 nm) and green (c. 550 to 570 nm) spectral regions (Dall'Olmo et al., 2005) because of strong absorption in the blue spectral region by dissolved organic matter, tripton, and phytoplankton pigments in turbid waters. Similarly in Lake Taihu, it has been shown that the natural logarithm of chlorophyll *a* concentration is closely related to the ratios R_{705}/R_{675} (Shu et al., 2000), R_{702}/R_{685} (Yang et al., 2005) and R_{706}/R_{682} (Ma & Dai, 2005a), where R is the reflectance and the number is the wavelength. Jiao et al. (2006) found that R_{719}/R_{670} had the greatest precision for retrieval of the chlorophyll *a* concentration of Lake Taihu while Wei et al. (2007) found that the chlorophyll *a* concentration in summer was well correlated with the Normalized Difference Vegetation Index (i.e., NDVI) of R_{696} and R_{661}. A regionally specific model was used by Ma et al. (2006), dividing the lake into several areas, and use bio-optical models for each location. Le et al. (2008) found in seasonal chlorophyll *a* retrieval models that the band ratios of R_{705}/R_{668} and R_{703}/R_{667} gave better results in spring and autumn, respectively. A four-band algorithm $[R^{-1}(662) - R^{-1}(693)]/[R^{-1}(740) - R^{-1}(705)]$ has also been developed to attempt to remove the absorption effect of suspended solids and associated partial suppression of water absorption in turbid waters (Le et al., 2009b).

It should be noted that all of these results were achieved using specialized optical measurements in the lab/field and not using satellite data directly. Considering the bandwidth of satellite remote sensing and atmospheric interference, it is difficult to extend special theoretical algorithms to satellite measurements directly (Gitelson et al., 2009). The parameterization of bio-optical properties is the main factors hindering the use of bio-optical algorithms using satellite measurements in Case 2 waters. In Lake Taihu, field measurements and radiative transfer simulation of bio-optical properties, including inherent optical properties (IOPs) and apparent optical properties (AOPs) have previously been conducted (Li et al., 2006; Le et al., 2009a; Zhang et al., 2009). These studies have required in situ measurements continued over a long period of time and covering the whole lake.

Recently, several approaches based on a spectral mixing modeling approach have been proposed to derive the chlorophyll *a* concentration of turbid lakes (Svab et al., 2005; Tyler et al., 2006; Oyama et al., 2009). The spectral mixing modeling approach, coupled with a multivariate (end member) regression analysis can be used to derive accurate estimates of chlorophyll *a*. The accuracy of these approaches depends on good end member selection, and screening of end members from one image cannot be applied to another image directly, which may affect the application of the approach for time series images.

The usefulness of these empirical algorithms for Case 2 waters could be improved by use of appropriate wave bands (IOCCG, 2000). Some researchers (Gitelson, 1992; Dall'Olmo et al., 2005; Duan et al., 2008) consider that pigment-based algorithms in high chlorophyll Case 2 waters can be improved by using longer wavebands (i.e., red and the near infrared spectral regions) than the typical blue and green bands used in Case 1 waters. Until bio-optical property and hyperspectral datasets become available for Lake Taihu, the empirical algorithms are still practical and effective for application of satellite data for assessment of the temporal–spatial chlorophyll *a* concentration (Ma & Dai, 2005b).

Our study was conducted to: (1) achieve a common empirical chlorophyll *a* concentration algorithm that could be used to retrieve the chlorophyll *a* distribution in Lake Taihu by correlating the in situ chlorophyll *a* data collected during 2005 with synchronous MODIS surface reflectance data; (2) monitor the synoptic distribution of chlorophyll *a* in Lake Taihu from 2006 to 2008 and reveal the spatial variability of chlorophyll *a*; and (3) examine the temporal and spatial variability of remotely sensed chlorophyll *a* in Lake Taihu from 2006 to 2008 using empirical orthogonal function (EOF) analysis.

Data and methods

Study site

Lake Taihu is located between 30°55′40″ to 31°32′58″N and 119°52′32″ to 120°36′10″E. The length of the lake (from north to south) is 68.5 km and the width (from east to west) is 56 km. The mean depth of the lake is 1.9 m, and the maximum depth is 2.6 m. The lake bottom has a flat terrain with an average topographic gradient of 0°0′19.66″ and an elevation of 1.1 m above sea level. The area of shallow-water with a mean depth <1.5 m is about 452 km^2, most of which is found in East Lake Taihu and accounts for 19.3% of the total surface area. The deepest areas (>2.5 m) are in the north and west, occupying 197 km^2 or 8.4% of the total lake area (Qin et al., 2007).

In situ data

A total of 28 stations (shown in Fig. 1) was sampled on the entire lake. Field measurements were collected at 13–28 stations once a month during 2005 by the Taihu Ecosystem Research and Field Observation Station of the Chinese Academy of Sciences. Samples for chlorophyll *a* were filtered on GF/C filters (Whatman) and chlorophyll *a* was extracted with ethanol (90%) at 80°C and analyzed spectrophotometrically at 750 and 665 nm, with correction for phaeopigments (Chen & Gao, 2000). There were 173 samples collected from the lake during 2005 at times when there was limited or no cloud cover.

Satellite data

MODIS-Terra surface reflectance level 2 products (MOD09) with a daily frequency and with a spatial resolution of 250 and 500 m bands covering the region of interest from 2005 to 2008 were downloaded via the web interface of the Land Processes Distributed Active Archive Center (LP DAAC) of NASA using the Warehouse Inventory Search Tool (WIST). The MODIS 250 and 500 m bands, especially at the visible and near infrared range, provide sufficient sensitivity for water applications, even though they were originally designed as "sharpening" bands for land studies and cloud detection (Hu et al., 2004). Five bands (band 1: 620–670 nm;

band 2: 841–876 nm; band 3: 459–479 nm; band 4: 545–565 nm; band 5: 1230–1250 nm) were used to retrieve the chlorophyll *a* concentration in Lake Taihu in this study. A total of 54 images from 2006 to 2008 that were (quasi-) synchronous with in situ data were selected to analyze the temporal and spatial variability of the algal blooms.

Pre-processing of MODIS images

Each image was re-projected onto the WGS 84 UTM zone 51 North coordinate system using the MODIS Reprojection Tool. The 500 m resolution images were resized to 250 m by the nearest neighbor method during re-projection.

The MOD09 product provides estimation of the surface spectral reflectance for each band as it would have been measured at ground level if there were no atmospheric scattering or absorption (Vermote et al., 2002). The quality of the atmospheric correction algorithm is strongly driven by the aerosol optical thickness (τ_a). For MODIS products, there is a climatological dataset of τ_a, and if an accurate τ_a is available, aerosol climatological data are replaced by an atmospheric correction algorithm, while the climatological data are still used when there are spatial and temporal gaps in τ_a (Vermote & Vermeulen, 1999; Vermote et al., 2002).

The surface reflectance of Lake Taihu is more accurate when τ_a is derived from MODIS products. Gaps sometimes exist in τ_a over Lake Taihu, however, thus some of the images are patchy and the surface reflectance from MOD09 could not be used directly in our research. Some areas therefore had to be re-corrected with τ_a obtained from climatological data. The quality description file of the MOD09 product (QA) includes aerosol retrieval information, which is important for re-correction. To examine the re-correction in detail, we used an image obtained on day 141 of 2008.

Figure 2 shows the grey-scale image of band 2, from which two different regions in Lake Taihu can be found. The state QA descriptions indicate that the aerosol parameters of region 1 and region 2 are climatology (mean of τ_a) and high, which means that there exists a gap of τ_a in region 1. Therefore, in our study, we used region 2 as the reference and adjusted the surface reflectance of region 1 to match that of region 2. To accomplish this, a simple relative normalization technique, Mean–Standard deviation (MS) normalization, was employed. This method is used to reduce the numeric differences between two images caused by disparities in the acquisition conditions such as sensor performance, solar irradiance, and atmospheric effects (Yuan & Elvidge, 1996). Two reference zones were used to achieve the correction parameters. Considering that the water quality of the two reference zones should be uniform, these two reference zones should be conjoint, and the distance between every reference zone and boundary should be limited to no more than one pixel (250 m). If R_{region1} and R_{region2} are the band reflectance of the two regions, $\bar{R}_{\text{zone1}}$ and $\bar{R}_{\text{zone2}}$ are the reflectance means of the two reference zones, and S_{zone1} and S_{zone2} are the standard deviations, then the MS coefficients are derived as:

$$m = \frac{S_{\text{zone2}}}{S_{\text{zone1}}} \quad b = \bar{R}_{\text{zone2}} - m\bar{R}_{\text{zone1}} \qquad R_{\text{region2}} = mR_{\text{region1}} + b \tag{1}$$

For this example, every reference zone was composed of 121 pixels chosen around different boundaries. $\bar{R}_{\text{zone1}}$ and $\bar{R}_{\text{zone2}}$ have values of 0.0996 and 0.00216, and S_{zone1} and S_{zone2} are 0.00350 and

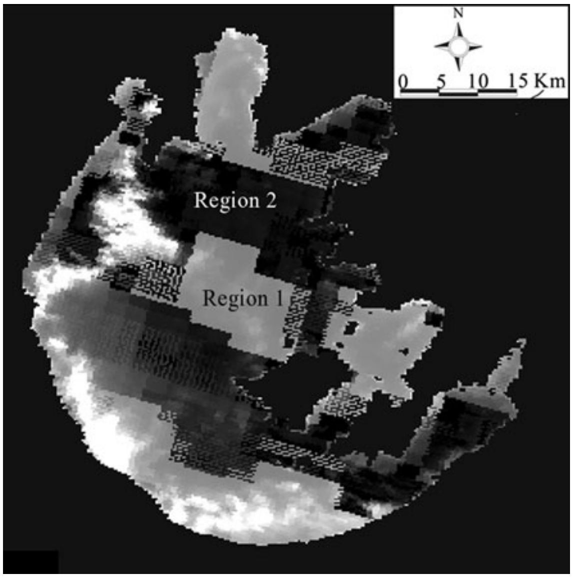

Fig. 2 Grey-scale image of MOD09 product (wavelength: 841–876 nm) showing Lake Taihu on day 141 of 2008. Aerosol optical thickness (τ_a) of annotated "region 1" is from the climatological dataset, where there exist spatial and temporal gaps of τ_a in this area; τ_a of annotated "region 2" is high and derived from MODIS aerosol products directly

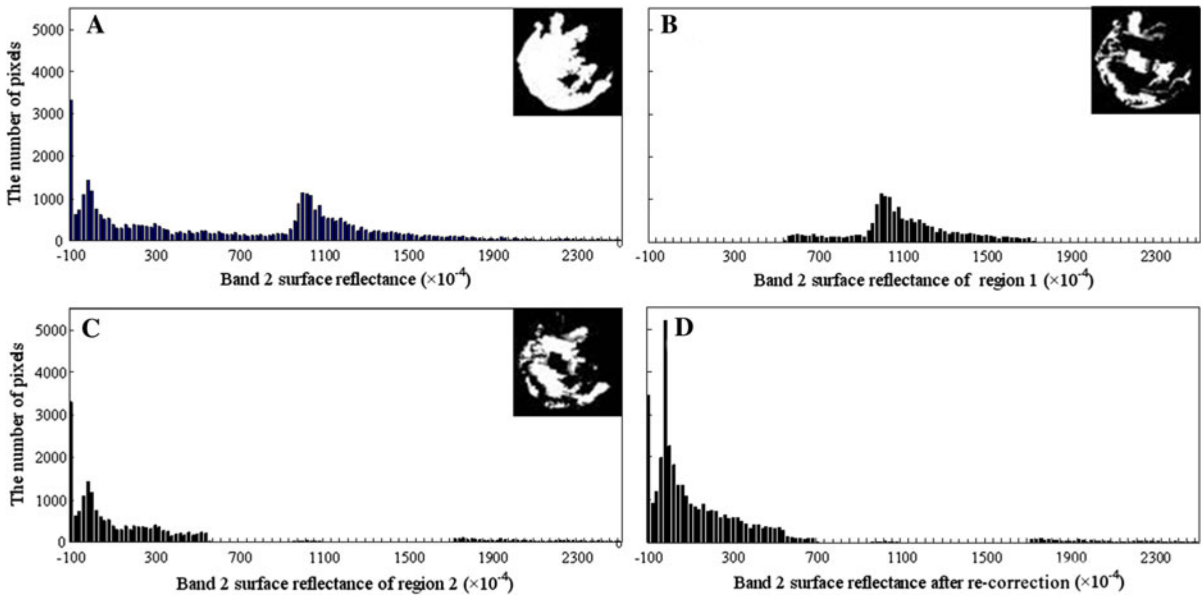

Fig. 3 Illustration of Mean–Standard Deviation method utilized in re-correction transformation. Statistical histograms of pixel numbers (250 m spatial resolution) are shown for the whole lake (**A**), region 1 (**B**) and region 2 (**C**), according to band 2 surface reflectance before re-correction; **D** is the histogram of pixel numbers in the whole lake after re-correction

0.00299, respectively. The slope (m) and intercept (b) of Eq. 1 are 0.854 and −0.0829, respectively. Another 55 pairs of pixels were processed in this way in order to validate the method. The results showed that the mean reflectance of the 55 pixels in region 1 would change from 0.0984 to 0.00109 after MS normalization, which is close to the mean reflectance of the corresponding pixels (0.00495) in region 2. Accordingly, the surface reflectance of region 1 can then be re-corrected to the base of region 2 using these equations. Figure 3A–C show the band 2 surface reflectance histograms of the entire lake, region 1 and region 2, respectively. Figure 3D shows the histogram of surface reflectance for the entire lake after re-correction. These findings indicate that the MS method can remove the correction difference between these two regions caused by inaccurate aerosol parameters.

EOF analysis

Empirical orthogonal function analysis is a useful technique for compressing the spatial and temporal variability of time series data down to the most energetic statistical modes. This method of data reduction was first applied to geophysical data for the purpose of statistical weather prediction (Yoder et al., 2002; Navarro & Ruiz, 2006). Recently, there have been many examples of EOF analysis for ocean-color data and analysis of chlorophyll *a* (Yoder et al., 2002; Navarro & Ruiz, 2006).

In this study, the computationally efficient singular value decomposition (SVD) method was applied to conduct the EOF analysis, to obtain the eigenvalues and amplitudes of the spatial and temporal variance (Yoder et al., 2002; Navarro & Ruiz, 2006). The spatial and temporal variance of the dataset ($x_m(t)$), can be partitioned into modes (i), revealing spatial functions ($\Phi_i(m)$), with time-varying amplitudes ($a_i(t)$), that are also known as principle components, such that

$$x_m(t) - \sum_{i=1}^{N} [a_i(t)\Phi_i(t)] \qquad (2)$$

This means that the time-variation in the chlorophyll *a* concentration of each pixel is the summation of $\Phi_i(m)$ with $a_i(t)$, indicating how the spatial modes vary with time. Eigenvalues can be considered as the portion of the total variance explained by the EOF, where the sum of the variances in the data equals the sum of variance in the eigenvalues (Yoder et al., 2002).

$$\sum_{m=1}^{M}\left\{\frac{1}{N}\sum_{n=1}^{N}[x_m(t_n)]^2\right\}=\sum_{j=1}^{M}\lambda_j \quad (3)$$

The EOF method requires a dataset without any gaps in space or time series. Consequently, MODIS images in which the main portion of Lake Taihu was <5% of cloud pixels were used in the present study, with pixels covered by clouds being replaced by the average of the surrounding pixels prior to performing the EOF analysis.

The errors of the EOF analysis, $\delta\lambda$, can be estimated by (North et al., 1982):

$$\delta\lambda \approx \lambda\left(\frac{2}{n}\right)^{1/2} \quad (4)$$

where λ is the eigenvalue and n is the number of images used in the EOF analysis. In this study, 54 MODIS images were used, so $\delta\lambda \approx 0.1925\ \lambda$. The mode of spatial variance is considered significant only if the distance between λ and its nearest eigenvalue is bigger than the error associated with its eigenvalue $\delta\lambda$.

Results

Empirical retrieval algorithm of chlorophyll *a*

Table 1 shows the bivariate correlation analysis of the surface reflectance of five MODIS bands and the chlorophyll *a* concentration from 2005. A significant ($r = 0.871$, $n = 145$, $P < 0.01$) relationship, excluding the 28 points observed in Feb 2005, was observed between the chlorophyll *a* concentration and band 2 reflectance in the near infrared range. However, the reflectance of the visible light range was poorly correlated with the chlorophyll *a* concentration ($r = -0.027$ for band 1; $r = 0.182$ for band 3; $r = 0.195$ for band 4; $r = 0.468$ for band 5). And the two-band reflectance ratio was also tested. Table 2 shows the relatively poor correlations ($r < 0.445$) between the chlorophyll *a* concentration and two-band ratios.

Accordingly, the reflectance of band 2 was used for the retrieval model. Curve fits revealed that the chlorophyll *a* concentration showed better correlations with an exponent of three ($r^2 = 0.907$, $n = 145$) or two ($r^2 = 0.907$, $n = 145$) of band 2 reflectance. A combination of band 2 data and the second exponent of band 2 reflectance was used for the empirical retrieval model of chlorophyll *a* in Lake Taihu.

Based on the above results, an in situ dataset including 145 pairs of samples was used for the empirical model:

$$C_{chl} = 9.8 \times 10^3 R_{b2}^2 - 44.0R_{b2} + 9.168 \quad r^2 = 0.907 \quad (5)$$

where R_{b2} is the surface reflectance of MODIS band 2.

EOF results

The chlorophyll *a* distributions of Lake Taihu derived from the MODIS images were initially spatially resized from 250 m to 1 km to avoid areas of high EOF scattering. The eigenvalue and percentage distribution of the normalized variance explained by the top 12 modes of spatial distribution are shown in Fig. 4. The error estimation of EOF indicates that only the first four modes are significant, and these explain 54.0% of the total chlorophyll *a* variance. Figure 5 shows the chlorophyll *a* concentration distribution of Lake Taihu from 2006 to 2008 based on the empirical algorithm (Eq. 5) given above. During early spring, the chlorophyll *a* concentration of the south region increases first (Fig. 5), especially around the mouth of the Tiaoxi River (refer to Fig. 1). High chlorophyll *a* concentrations corresponding to algal blooms then move from south to north along the southwestern lakeshore, with Zhushan Bay, Meiliang Bay, and Gonghu Bay (Fig. 1) regularly having blooms from May to October. In winter, the region with high chlorophyll *a* concentrations changes from north to south along the southwestern lakeshore until bloom levels are no longer present.

Figure 6 shows the mean distribution of the chlorophyll *a* concentration derived from EOF analysis. It shows that the west and the north regions of Lake Taihu are characterized by relatively high chlorophyll *a* concentrations, and that large parts of the eastern region are covered by macrophytes. Figures 7 and 8 show the spatial maps and time series amplitude of the first four modes, respectively, which are useful in evaluating the seasonal and interannual chlorophyll *a* concentration spatial variability across the lake. The peak concentrations of chlorophyll *a* typically appeared during summer and

Table 1 Correlation coefficient values of the chlorophyll *a* concentration and MODIS band reflectance for five bands at 173 observation points in 2005

Date	Pearson coefficient (*r*)	Bands surface reflectance of MODIS				
		Band 1	Band 2	Band 3	Band 4	Band 5
28 samples for Feb	Chlorophyll *a* concentration	−0.676**	−0.660*	−0.588**	−0.646**	0.690**
	TSM concentration	0.702**	0.810**	0.574**	0.643**	−0.168
Remaining 145 samples	Chlorophyll *a* concentration	−0.027	0.871**	0.182*	0.195*	0.468**
	TSM concentration	0.646**	0.261**	0.358**	0.475**	−0.105

** $P \leq 0.01$ (2-tailed *t* test); * $P \leq 0.05$ (2-tailed *t* test)

Table 2 Correlation coefficient values of the chlorophyll *a* concentration and reflectance band ratios for 145 observation points in 2005

	Bands surface reflectance ratio of MODIS				
	R2/R1	R3/R1	R4/R1	R5/R1	R3/R2
Chlorophyll concentration	0.372**	0.240**	0.175*	0.379**	−0.409**
	R4/R2	R5/R2	R4/R3	R5/R3	R5/R4
Chlorophyll concentration	−0.445**	0.052	−0.021	0.174*	0.339**

** $P \leq 0.01$ (2-tailed *t* test); * $P \leq 0.05$ (2-tailed *t* test)

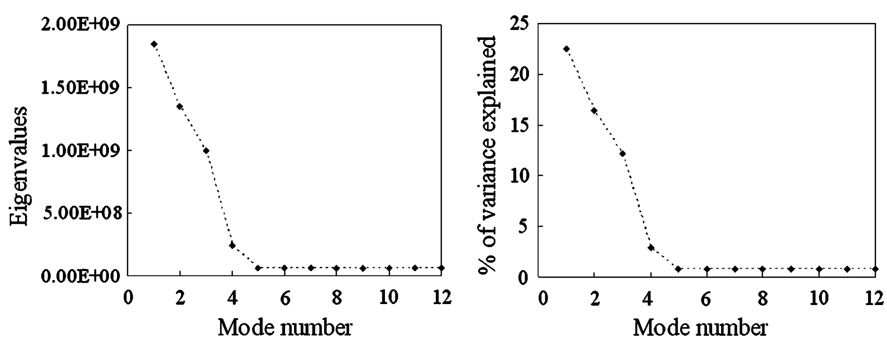

Fig. 4 Eigenvalue and percent of variance explained by the EOF modes

autumn, while the minimum concentrations were observed during winter and early spring.

Figure 9 shows a scatter plot of 173 observation points that indicates that the chlorophyll *a* concentration of the measurement points relates very well to the surface reflectance of band 2, excluding the 28 points observed in Feb 2005. The relationship between the chlorophyll *a* concentration and band 2 reflectance of the remaining 145 points is much different from that of the 28 points for Feb. For Lake Taihu, as chlorophyll *a* increases, the reflectance spectrum is increasing dominated by chlorophyll *a* over TSM and CDOM.

Comparison of the coincident satellite and in situ observations (50 samples) from December of 2008 to September of 2009 provided estimates of the accuracy and precision of the empirical algorithm. The locations of the samples were THL 04, 08, 10, 13, 16, 18, 19, 22, and 24 (Fig. 1). Chlorophyll *a* concentrations of samples were measured using the same methods as those for the 2005 dataset. We calculated the relative error (RE) and root mean square error (RMSE) between the predictions and observations using the following equations:

$$\mathrm{RE} = \left[\left|C_{\mathrm{pred}}/C_{\mathrm{in\,situ}} - 1\right| \cdot 100\right]\% \quad (6)$$

$$\mathrm{RMSE} = \left[\sum \left(C_{\mathrm{pred}} - C_{\mathrm{in\,situ}}\right)^2/n\right]^{0.5} \quad (7)$$

where C_{pred} is the concentration predicted from the retrieval algorithm, $C_{\mathrm{in\,situ}}$ represents the concentration measured in the lab, and n is the number of samples.

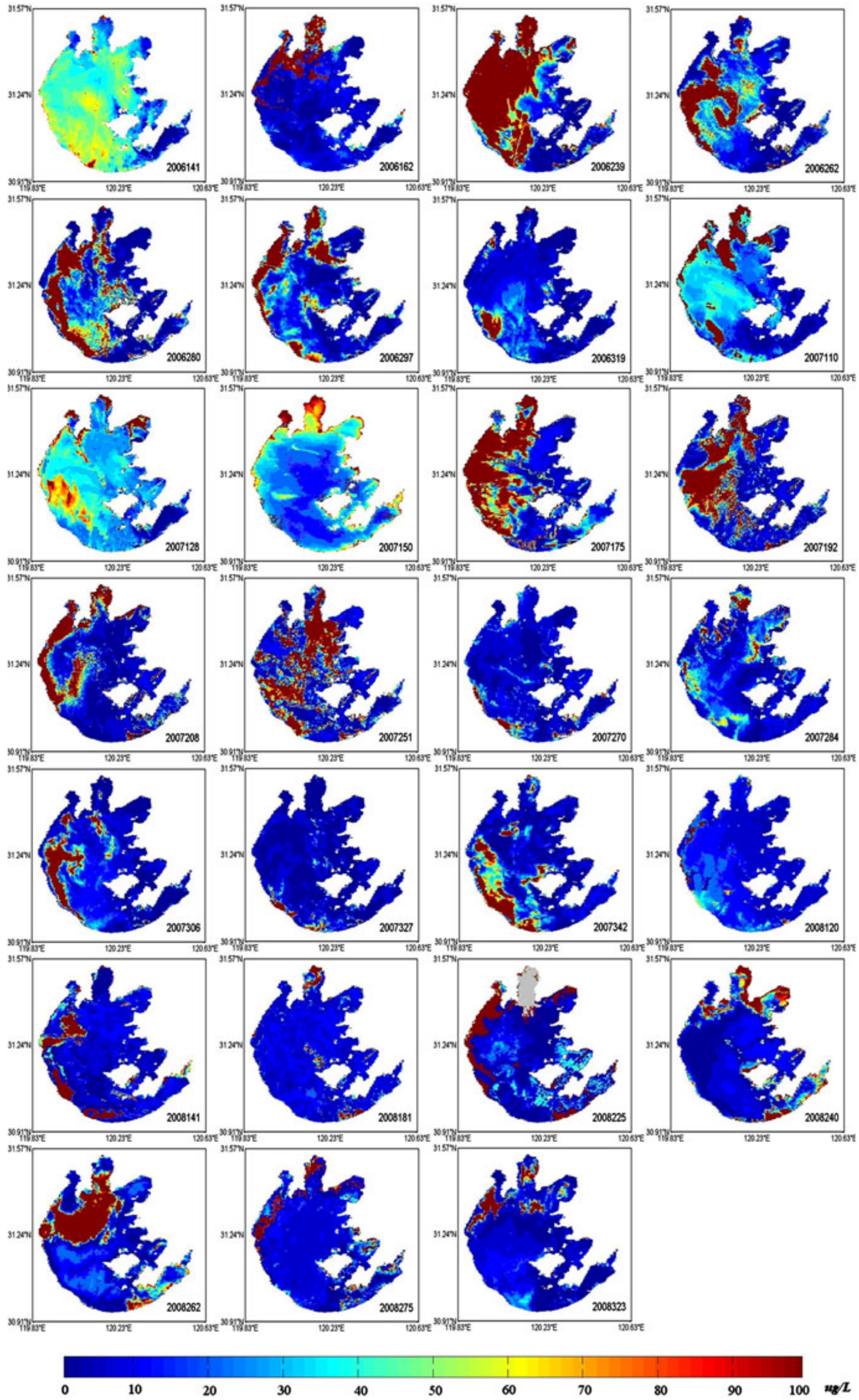

Fig. 5 Algal blooms definition in Lake Taihu from 2006 to 2008 derived from MODIS images. *Grey* area represents missing values covered by cloud

Figure 10 shows a comparison of the calculations and observations of the 2005 dataset, and the 2008–2009 dataset. The chlorophyll *a* concentration of the two datasets ranged from 1.39 to 119.9 μg/l and 1.8 to 290.3 μg/l, respectively, while the RMSE for these two datasets was 6.28 and 7.48 μg/l. Figure 11 shows chlorophyll *a* concentration versus RE for the two datasets. The RE values of the 2005

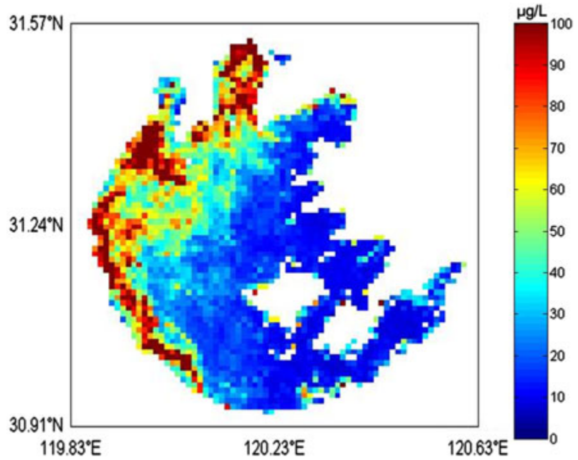

Fig. 6 Mean chlorophyll *a* concentration derived from the MODIS data

and 2008–2009 datasets were 36.9 and 61.3%, respectively. When the chlorophyll *a* concentration was <10 µg/l, the RE values of the modeled and validated data were 62.1 and 83.8%, respectively. When the chlorophyll *a* concentration was ≥10 µg/l, the RE values were only 25.2 and 30.4%, respectively.

Discussion

MODIS bands retrieving chlorophyll *a*

Due to the high absorption of TSM and CDOM in the blue–green range, the absorption of phytoplankton in the blue range is weak and ability to quantify chlorophyll *a* is reduced (Yu et al., 2003). Conversely, in the near infrared range, the absorption of TSM and CDOM becomes very weak, and the reflectance in this range is useful for color remote sensing of phytoplankton. Duan et al. (2008) also considered MODIS band 2 to be the best band to distinguish algal blooms and water in Lake Taihu. The reflectance of algal blooms in the near infrared (NIR) range is much different from that of water, and resembles the reflectance of vegetation, especially the steep slope effect of vegetation (Duan et al., 2008).

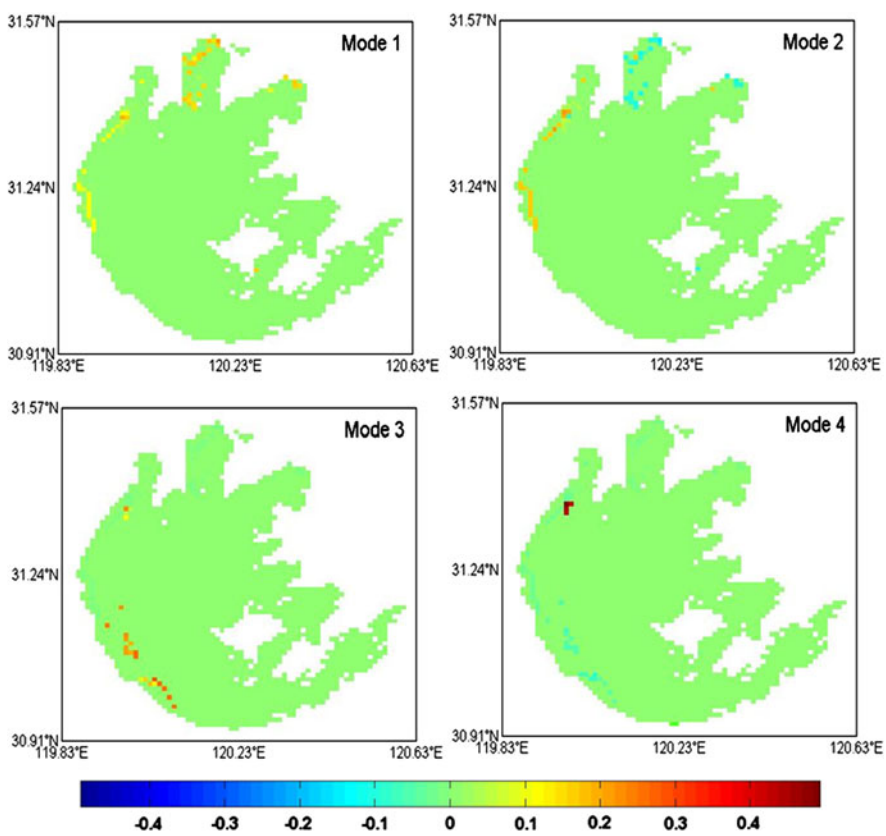

Fig. 7 First four modes of spatial distribution obtained from EOF analysis

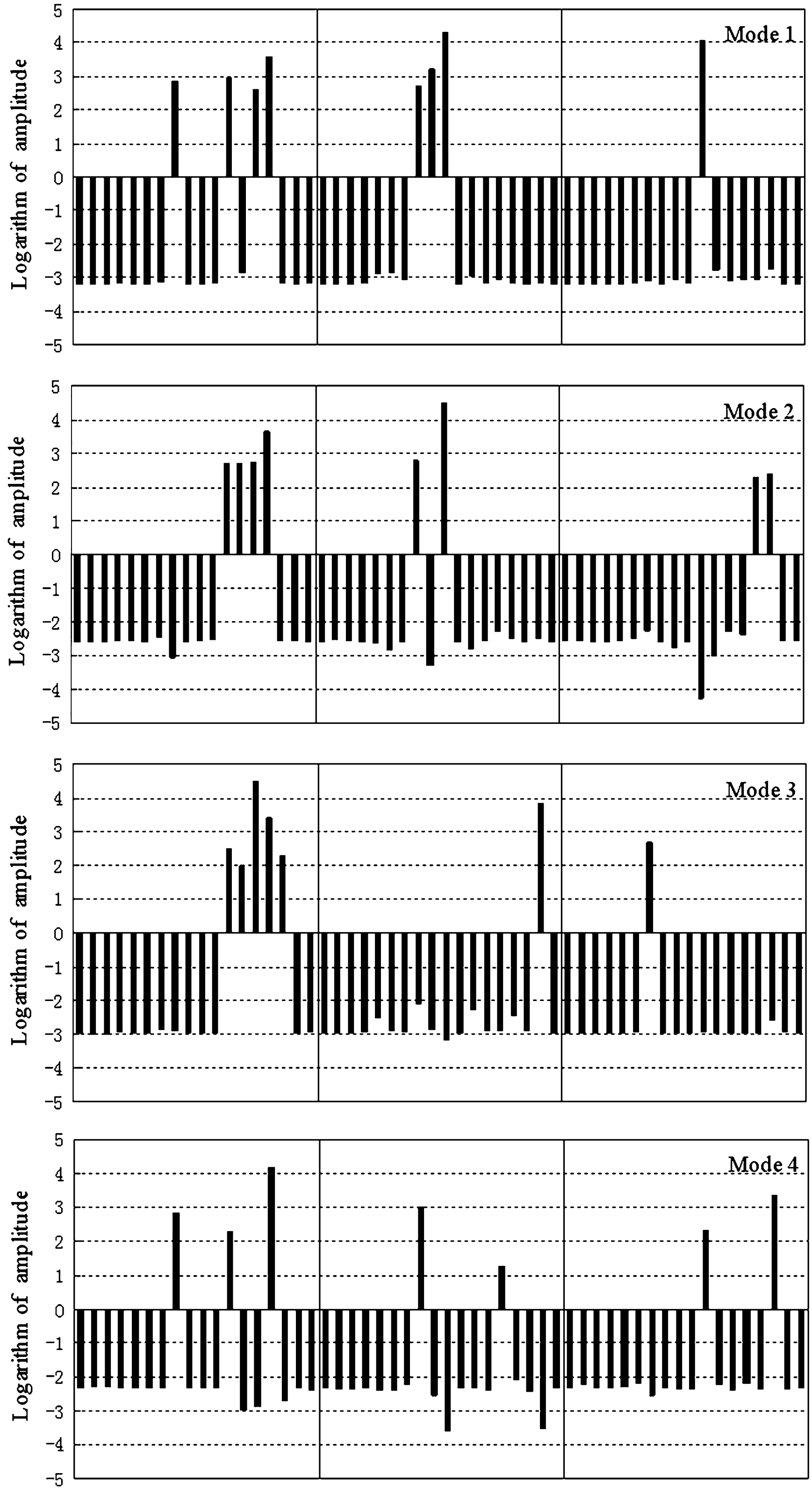

Fig. 8 Time series amplitude of the first four modes of spatial distribution obtained from EOF analysis

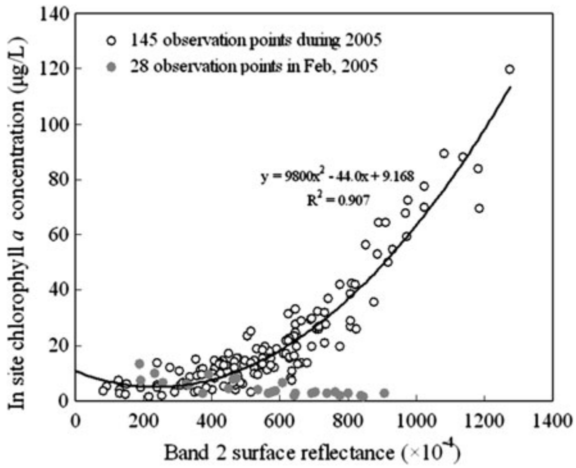

Fig. 9 Relationship between band 2 surface reflectance and chlorophyll *a* concentration of 173 observation points in 2005. *Thick line* is a quadratic regression only for 145 observation points

For the data of Feb 2005, the wind velocity at the observation time was >4.2 m/s, which likely caused a high concentration of total suspended materials (TSM) (≥200 mg/l). The spectral reflectance increases in the visible spectrum in turbid waters, especially in the red portion (ca. 600–700 nm). The common method used to relate remotely sensed reflectance in the red portion to TSM concentration is reasonably robust in coastal and inland waters because scattering from suspended materials frequently dominates the reflectance spectra when compared to pure water and phytoplankton absorption (Miller & McKee, 2004). While the chlorophyll *a* concentration of Lake Taihu is relatively low during winter (≤10 μg l^{-1}), the reflectance spectrum is dominated by TSM and CDOM (Yu et al., 2003).

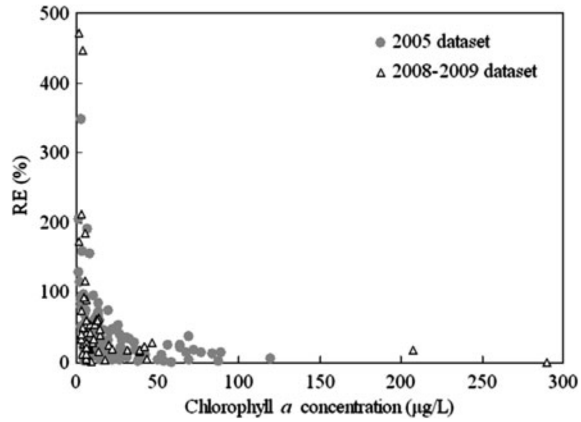

Fig. 11 Relationship between relative error (RE) and the scale of the chlorophyll *a* concentration

Moreover, a "red-shift" effect will occur when the TSM concentration is very high (Han & Rundquist, 1994). Therefore, for the 28 points observed in Feb, not only reflectance of bands in the visible range but also band 2 in the near infrared range was correlated well with the TSM concentrations (Table 1). Accordingly, the empirical algorithm (Eq. 5) using band 2 of MODIS could not be applied when the TSM concentration was very high (≥200 mg l^{-1}).

Influence of the bottom on water color

In shallow waters, the reflected radiance from the water can have an additional component: light reflected off the bottom. The maximum depth from which the sensor receives any significant signal varies as a function of wavelength and with the clarity of the water (IOCCG, 2000). The Secchi depths of Lake Taihu are normally low, i.e., about 30–40 cm in the

Fig. 10 Scatterplot of retrieved and measured chlorophyll *a* concentration for 2005 dataset (**A**) and 2008–2009 dataset (**B**). The *thick line* is 1:1 relationship

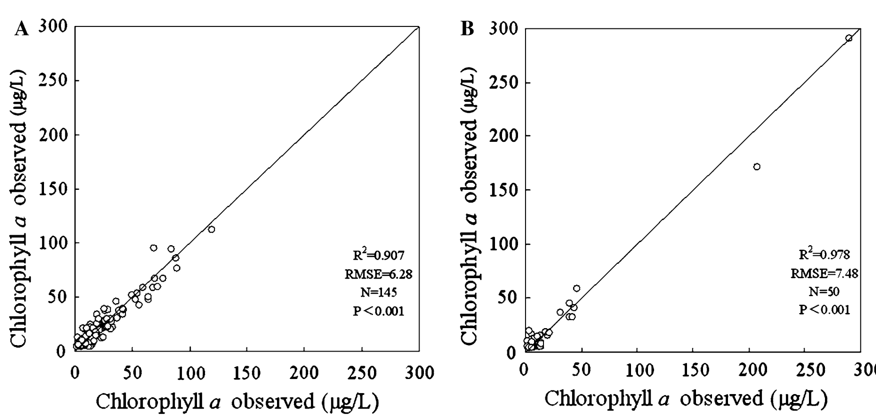

north and 40–50 cm in the south, and underwater irradiance measurements have shown that the irradiance at 1 m is about 10% of that at the surface (Qin et al., 2007). Furthermore, water quality of the eastern lakeshore and East Lake Taihu is relatively clear and water depth is about 1 m. Accordingly, in these areas the bottom can affect the accuracy of the empirical algorithm, and the mean RE of samples in the eastern lakeshore and East Lake Taihu were as high as 61.9%. Nevertheless, the RMSE of the samples located in these regions was only 2.92 μg l^{-1}. The performance of the empirical model in the bottom-influenced area is acceptable when optical properties are unavailable for the region.

EOF analysis of chlorophyll *a* distribution

Seasonal variability

The first mode of spatial distribution responsible for 22.5% of the normalized variance of spatial distribution showed that there was high variation in chlorophyll *a* in Meiliang Bay and along the north lakeshore of Gonghu Bay as well as in the west and northwest shore of the lake and low values ($\leq$10 μg l^{-1}) were observed over the center and eastern portion of the lake. The amplitude of the time series indicates that this pattern is modulated by the general seasonal cycle and inter-annual variability. Most of the spatial coefficients of the first mode were positive (Fig. 7), consequently, when they were multiplied by positive temporal amplitudes of the first mode, the entire field of Lake Taihu increased with respect to the chlorophyll *a* climatology, while negative amplitudes resulted in a decrease in the field (Navarro & Ruiz, 2006). High values occurred in fall (September/October) of 2006, in summer (June/July) of 2007, and in the fall and early winter of 2008, with the 2007 summer peak of chlorophyll *a* concentrations being the highest observed during the study period.

The second mode of spatial distribution explained 16.4% of the normalized variance (Fig. 7). The spatial distribution of this mode allowed us to distinguish three different zones throughout the lake. The first zone was located in the open lake and eastern portion of Lake Taihu, and was characterized by values of the spatial coefficient near 0, which indicates a high stability of the surface chlorophyll *a*. The second area included Meiliang Bay and Gonghu Bay and was characterized by negative coefficients, suggesting the existence of a phytoplankton bloom when the temporal amplitude was also negative. The hydrodynamics of Lake Taihu during summer result in a stable southward current along the western coast and an unstable current in Meiliang Bay (Luo & Qin, 2004; Hu et al., 2004). In addition, there is a weak counter-clockwise current in the northern Meiliang Bay, regardless of the season (Qin et al., 2000; Luo et al., 2004a, b), which may explain why this area is favorable for concentrating algal blooms (Qin et al., 2000). In contrast, zone 3, which occupies the western lakeshore, was characterized by positive spatial modes, indicating that there is a dynamic response of wind-induced currents in Lake Taihu.

The characteristics of the third and fourth mode (12.1 and 2.9% of the variance, respectively) are similar to those of the first mode and the second mode, respectively. These two modes capture the high variability during the late spring or early winter period, which is primarily along the southwestern lakeshore. This spatial pattern was relatively weak in 2008, but intensified in 2007. During summer, the prevailing wind from the southeast or southwest can generate a counter-clockwise water current in the center of the lake, and there is a southward current along the western and southern coast (Qin et al., 2000). Accordingly, algal blooms may be move from the north area to the southern lakeshore by this current before the arrival of winter. Conversely, the phytoplankton may be shifted from the south to the north by the opposite current.

Variability among regions

The chlorophyll *a* spatial distribution of the first two modes corresponds to algal blooms along the western lakeshore, in Meiliang Bay and in Gonghu Bay. These findings indicate that algal blooms always occur in these two bays during summer, whereas chlorophyll *a* may increase from early summer to late fall along the western lakeshore. The temporal characteristics of the southwestern lakeshore could be derived from the third and fourth modes, which show that algal blooms occur during the early summer and fall, and sometimes during early winter in this area. Furthermore, the remaining regions, including the center of the lake, the eastern lakeshore and East Taihu, exhibit relatively stable chlorophyll *a* concentrations.

Inter-annual variability

The inter-annual variance analysis shown in Fig. 8 indicates that algal blooms occurred during late summer and fall of 2006. In 2008, the region of high chlorophyll *a* was similar to that of 2006, but the timing was shifted to summer and early spring. During 2007 the duration of the algal bloom-covered area was from April to December.

Table 3 shows the statistical results for areas of high chlorophyll *a* concentration ($\geq$100 μg l^{-1}) in Lake Taihu from 2006 to 2008, and Fig. 12 shows the time-series comparison over 3 years of high chlorophyll *a* concentration areas amongst eight regions of Lake Taihu. The largest area of high chlorophyll *a* was on day 239 of 2006, and was about 1,100 km^2, or half of the entire lake. Ma et al. (2008) also found that since 2003, algal blooms in Lake Taihu occurred in the center of the lake, as well as in bays and near lakeshores, and that they occasionally covered almost the entire non-vegetation area. Blooms occurred in early May of 2006 and 2008, whereas they occurred in late March in 2007. Surprisingly, the duration of water blooms was greatest in 2007, lasting from early spring until winter. Furthermore, algal blooms always disappeared during late June, and this phenomenon was strong in 2006 and 2008 and weak in 2007. Generally, the rainy season begins in late June and lasts for at least several days. During this period solar radiation is low, which affects the growth of algae (Kong & Gao, 2005).

Implications for lake management

Due to the complexity of the causes of algal blooms, development of an integrated lake management system requires not only the most robust and effective

Table 3 Area (km^2) of high chlorophyll *a* concentration ($\geq$100 μg l^{-1}) in Lake Taihu derived from Eq. 5

Time	Zhushan Bay	Meiliang Bay	Gonghu Bay	Western lakeshore	Southern lakeshore	Center of the lake	East area
2006							
Maximum	45	97	25	273	133	502	25
Average	6.11	15.89	2.11	39.67	22.44	57.50	5.89
2007							
Maximum	39	82	34	225	131	321	35
Average	7.26	22.11	7.63	37.84	31.74	61.85	7.79
2008							
Maximum	16	101	44	113	125	311	58
Average	1.44	16.25	7.38	25.63	21.63	33.13	13.06

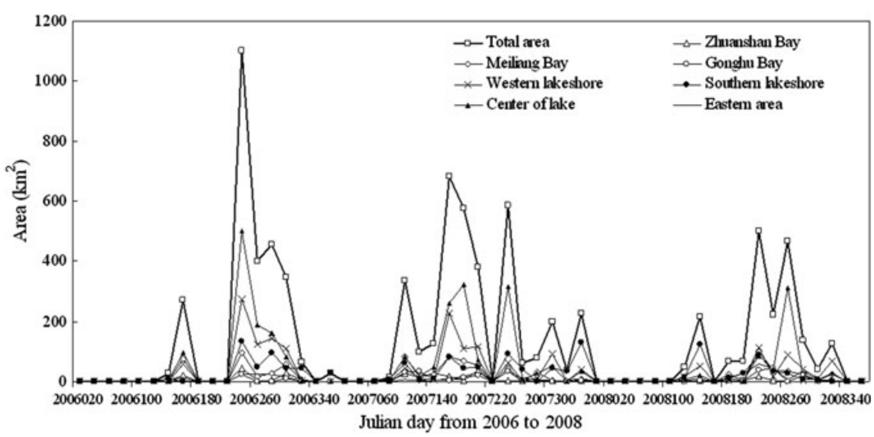

Fig. 12 Time-series comparison of algal bloom area in eight regions of Lake Taihu for 3 years (2006–2008). The location of these eight regions is shown in Fig. 1

techniques, but also systems analysis. In Lake Taihu, many engineering projects have been undertaken by the Chinese government to control algal blooms (Wang et al., 2006).

For the restoration projects in the littoral zone, appropriate location selection could improve the effectiveness of the projects. According to the results mentioned above, the west and southwest coast, the north lakeshore of Gonghu Bay and the entire lakeshore of Meiliang Bay could be selected as the preferred sites for regeneration projects such as the establishment of wetlands and riparian zones.

Water transfer from the Yangtze River to Lake Taihu is a large-scale project executed from 2002 to increase water circulation in the lake and rivers. For this project, Yangtze River water is pumped and channeled through the Wangyu River and discharged into Gonghu Bay. But the results of EOF also showed that during the diversion, the concentrated cyanobacterial was flushed into the northern lakeshore of Gonghu Bay, where it entered the Wuxi drinking water plant (Qin et al., 2010). Therefore, the effect of water diversion in such a large lake would likely not be as expected. This project should be viewed as a temporary measure to improve water quality of some regions, and it should be noted that this project may lead to new ecological and environmental problems in the downstream and coastal areas.

The water source of the Wuxi drinking water plant is located near the north lakeshore of Gonghu Bay, which has been demonstrated to be a region of high chlorophyll *a* and is therefore a high-risk region for algal blooms. Indeed, an algal bloom event resulted in a major crisis that directly affected water supply for approximately 2 million people (Qin et al., 2010). Considering the water quality around Wuxi is unsatisfactory, it is necessary to strengthen the management of the water source protection zone, improve the capability of the emergency response and establish an early warning system to ensure water quality.

The wind direction and velocity are key factors that influence the temporal and spatial distribution of algal blooms (Kong & Gao, 2005). The first four modes of our EOF analysis demonstrate that chlorophyll *a* is concentrated to the leeward region of the prevailing wind direction. Furthermore, extremely warm weather combined with local wind conditions favor bloom expansion (Qin et al., 2010). Studies have suggested that the Lake Taihu area will experience continued spring (March–May) warming, with increases ranging from 0.21 to 0.89°C occurring over the next decade (2010–2019) when compared to the previous four decades (1960–2000) (Qin et al., 2010). These findings suggest that algal blooms will likely recur earlier than historically observed in this lake (Chen et al., 2003; Zhu, 2008). According to the seasonal variability results from EOF analysis, algal blooms maybe take place along the southwestern lakeshore first. Therefore, during the late spring and early winter the southwestern coast should be the concern of the lake management administration of Lake Taihu, while the western part of the lake will become a high-risk area of algal blooms from summer to fall.

Conclusions

A common empirical retrieval model of the chlorophyll *a* concentration in Lake Taihu was developed using the results of in situ measurement and synchronous MODIS images from 2005. The synoptic distribution of chlorophyll *a* in Lake Taihu from 2006 to 2008 was then obtained using this algorithm and the time series MODIS data. EOF analysis was then conducted to obtain the temporal and spatial distributions of chlorophyll *a* and algal blooms in Lake Taihu.

The time-series chlorophyll *a* distribution of Lake Taihu from 2006 to 2008 and the mean distribution of the chlorophyll *a* concentration derived from EOF analysis show that the west and north regions are characterized by relatively high chlorophyll *a* concentrations, and the eastern region has relatively low chlorophyll *a*. In addition, the concentration peaks of chlorophyll *a* typically appeared in summer and autumn while the minima occurred during winter and early spring. The first four modes of EOF explain 54.0% of the total chlorophyll *a* variance and can be used to represent the spatial extent and temporal variability of the processes in the study area. The amplitude of each mode differed among the 3 years examined.

Different regions of variability indicate that during the summer algal blooms always occur in Meiliang Bay and Gonghu Bay, while they occur around the southwestern lakeshore during summer and fall, and even early winter. The remaining regions, including the center of the lake, east lakeshore and eastern portion of Lake Taihu, exhibit relatively low variance of chlorophyll *a* concentration at the water surface.

The largest area of high chlorophyll *a* concentration ($\geq$100 μg l^{-1}) was on day 239 of 2006. The year 2007 was different from 2006 and 2008, because the algal bloom-covered area was larger and the duration extended from April to December.

Although the accuracy and stability of our empirical model is satisfactory, theoretical retrieval algorithms for chlorophyll *a* are still preferable for Case 2 waters. The temporal and spatial distribution of algal blooms in Lake Taihu should be analyzed together with solar radiation, wind fields, hydrodynamics, and water quality distributions to enable an improved understanding of the environmental factors contributing to the spatial and temporal variations in chlorophyll *a* in the lake.

Acknowledgments We are grateful to NASA for providing the MODIS-Terra surface reflectance daily level 2 products (MOD09), and to the Taihu Ecosystem Research and Field Observation Station, Chinese Academy of Sciences, for providing field measurement data. This study was funded by the National Basic Research Program of China (“973” Program), 2008CB418003, the National High Technology Research and Development Program of China, 2007AA06A405, and the Chinese National Science Foundation, 40701005. We thank Associate Prof. Heng Lu from Nanjing Normal University for his helpful advice and we thank two anonymous reviewers for their careful reviews and constructive suggestions.

References

Chen, Y. W. & X. Y. Gao, 2000. Comparison of two methods for phytoplankton chlorophyll-*a* concentration measurement. Hupo Kexue 12: 185–188 (in Chinese).

Chen, Y. W., C. X. Fan, K. Teubner & M. Dokullil, 2003. Changes of nutrients and phytoplankton chlorophyll-*a* in a large shallowlake, Taihu, China: an 8-year investigation. Hydrobiologia 506: 273–279.

Dall’Olmo, G., A. A. Gitelson, D. C. Rundquist, B. Leavitt, T. Barrow & J. C. Holz, 2005. Assessing the potential of SeaWiFS and MODIS for estimating chlorophyll concentration in turbid productive waters using red and near-infrared bands. Remote Sensing of Environment 96: 176–187.

Duan, H., S. Mang & Y. Mang, 2008. Cyanobacteria bloom monitoring with remote sensing in Lake Taihu. Hupo Kexue 20: 145–152 (in Chinese).

Gitelson, A., 1992. The peak near 700 nm on radiance spectra of algae and water relationships of its magnitude and position with chlorophyll concentration. International Journal of Remote Sensing 13: 3367–3373.

Gitelson, A. A., D. Gurlin, W. J. Moses & T. Barrow, 2009. A bio-optical algorithm for the remote estimation of the chlorophyll-*a* concentration in case 2 waters. Environmental Research Letters 4: 045003.

Han, L. H. & D. C. Rundquist, 1994. The response of both surface reflectance and the underwater light field to various levels of suspended sediments – preliminary results. Photogrammetric Engineering and Remote Sensing 60: 1463–1471.

Hu, C. M., Z. Q. Chen, T. D. Clayton, P. Swarzenski, J. C. Brock & F. E. Muller-Karger, 2004. Assessment of estuarine water-quality indicators using MODIS medium-resolution bands: initial results from Tampa Bay, FL. Remote Sensing of Environment 93: 423–441.

Hu, W. P., S. E. Jorgensen & F. B. Zhang, 2006. A vertical-compressed three-dimensional ecological model in Lake Taihu, China. Ecological Modelling 190: 367–398.

IOCCG, 2000. Remote sensing of ocean colour in coastal, and other optically-complex, waters. In Sathyendranath, S. (ed.), Reports of the International Ocean-Colour Coordinating Group. IOCCG, Dartmouth, Canada.

Jiao, H. B., Y. Zha, Y. M. Li, J. Z. Huang & Y. C. Wei, 2006. Modelling chlorophyll-*a* concentration in Lake Taihu from hyperspectral reflectance data. Journal of Remote Sensing 10: 242–248 (in Chinese).

Kong, F. X. & G. Gao, 2005. Hypothesis on cyanobacteria bloom-forming mechanism in large shallow eutrophic lakes. Acta Ecologica Sinica 25: 589–595 (in Chinese).

Le, C. F., Y. M. Li, D. Y. Sun, H. J. Wang & C. C. Huang, 2008. Spatio-temporal distribution of chlorophyll *a* concentration and its estimation in Lake Taihu. Huanjing Kexue 29: 619–626 (in Chinese).

Le, C. F., Y. M. Li & Y. Zha, 2009a. Specific absorption coefficient and the phytoplankton package effect in Lake Taihu, China. Hydrobiologia 619: 27–37.

Le, C. F., Y. M. Li, Y. Zha, D. Y. Sun, C. C. Huang & H. Lu, 2009b. A four-band semi-analytical model for estimating chlorophyll *a* in highly turbid lakes: the case of Lake Taihu, China. Remote Sensing of Environment 113: 1175–1182.

Li, Y. M., J. Z. Huang, Y. C. Wei, W. N. Lu & J. Z. Shi, 2006. Evaluating eutrophic state of Lake Taihu by in situ hyperspectra. Huanjing Kexue 27: 1770–1775 (in Chinese).

Luo, L. & B. Qin, 2004. Numerical simulation based on a three-dimensional shallow-water hydrodynamic model-current circulations in Lake Taihu with prevailing wind-forcing. Journal of Hydrodynamics (Serial B) 16: 341–349.

Luo, L., B. Qin & G. Zhu, 2004a. Sediment distribution pattern mapped from the combination of objective analysis and geostatistics in the large shallow LakeTaihu, China. Journal of Environmental Sciences 16: 908–911 (in Chinese).

Luo, L., B. Qin, G. Zhu & Y. Zhang, 2004b. The current pattern of Meiliang Bay in the winter time. Hupo Kexue 16: 73–76 (in Chinese).

Ma, R. H. & J. Dai, 2005a. Chlorophyll-*a* concentration estimation with field spectra of water body near Meiliang Bay in Lake Taihu. Journal of Remote Sensing 9: 78–86 (in Chinese).

Ma, R. H. & J. F. Dai, 2005b. Investigation of chlorophyll-*a* and total suspended matter concentrations using Landsat ETM and field spectral measurement in Lake Taihu, China. International Journal of Remote Sensing 26: 2779–2795.

Ma, R., J. Tang & J. Dai, 2006. Bio-optical model with optimal parameter suitable for Lake Taihu in water colour remote sensing. International Journal of Remote Sensing 27: 4305–4328.

Ma, R., F. Kong, H. Duan, S. Zhang, W. Kong & J. Hao, 2008. Spatio-temporal distribution of cyanobacteria blooms based on satellite imageries in Lake Taihu, China. Hupo Kexue 20: 687–694 (in Chinese).

Miller, R. L. & B. A. McKee, 2004. Using MODIS terra 250 imagery to map concentrations of total suspended matter in coastal waters. Remote Sensing of Environment 93: 259–266.

Navarro, G. & J. Ruiz, 2006. Spatial and temporal variability of phytoplankton in the Gulf of Cadiz through remote sensing images. Deep-Sea Research Part II – Topical Studies in Oceanography 53: 1241–1260.

North, G. R., T. L. Bell, R. F. Cahalan & F. J. Moeng, 1982. Sampling errors in the estimation of empirical orthogonal functions. Monthly Weather Review 110: 699–706.

Oyama, Y., B. Matsushita, T. Fukushima, K. Matsushige & A. Imai, 2009. Application of spectral decomposition algorithm for mapping water quality in a turbid lake (Lake Kasumigaura, Japan) from Landsat TM data. ISPRS Journal of Photogrammetry and Remote Sensing 64: 73–85.

Qin, B., W. Hu, W. Chen, J. Ji, C. Fan, Y. Chen, X. Gao, L. Yang, G. Gao, W. Huang, J. Jiang, S. Zhang, Y. Liu & Z. Zhou, 2000. Studies on the hydrodynamic processes and related factors in Meiliang Bay, Northern Taihu. Hupo Kexue 12: 327–334 (in Chinese).

Qin, B. Q., P. Z. Xu, Q. L. Wu, L. C. Luo & Y. L. Zhang, 2007. Environmental issues of Lake Taihu, China. Hydrobiologia 581: 3–14.

Qin, B. Q., G. W. Zhu, G. Gao, Y. L. Zhang, W. Li, H. W. Paerl & W. W. Carmichael, 2010. A drinking water crisis in Lake Taihu, China: linkage to climatic variability and lake management. Environmental Management 45: 105–112.

Shu, X. Z., Q. Yin & D. B. Kuang, 2000. Relationship between algal chlorophyll concentration and spectral reflectance of inland waters. Journal of Remote Sensing 4: 41–45 (in Chinese)

Svab, E., A. N. Tyler, T. Preston, M. Presing & K. V. Balogh, 2005. Characterizing the spectral reflectance of algae in lake waters with high suspended sediment concentrations. International Journal of Remote Sensing 26: 919–928.

Tyler, A. N., E. Svab, M. Preston & W. A. Kovacs, 2006. Remote sensing of the water quality of shallow lakes: a mixture modelling approach to quantifying phytoplankton in water characterized by high suspended sediment. International Journal of Remote Sensing 27: 1521–1537.

Vermote, E. F. & A. Vermeulen, 1999. Atmospheric correction algorithm: spectral reflectance (MOD09). Algorithm Technical Background Document Version 4.0, NASA Goddard Space Flight Center, Greenbelt, MD 20771, USA.

Vermote, E. F., N. Z. El Saleous & C. O. Justice, 2002. Atmospheric correction of MODIS data in the visible to middle infrared: first results. Remote Sensing of Environment 83: 97–111.

Wang, Q. G., G. Gu & Y. Higano, 2006. Toward integrated environmental management for challenges in water environmental protection of Lake Taihu basin in China. Environmental Management 37: 579–588.

Wei, Y. C., J. Z. Huang, Y. M. Li & J. Guang, 2007. The hyperspectral data monitoring model of chlorophyll-*a* of summer in Lake Taihu, China. Journal of Remote Sensing 11: 756–762 (in Chinese).

Yang, D. T., D. L. Pan & X. Y. Zhang, 2005. Retrieval of water quality parameters by hyperspectral remote sensing in Lake Taihu, China, Spie-Int Society Optical Engineering. In: sings of the Society of Photo-Optical Instrumentation Engineers, Bellingham: 431–439.

Yang, M., J. W. Yu, Z. L. Li, Z. H. Guo, M. Burch & T. F. Lin, 2008. Lake Taihu not to blame for Wuxi's woes. Science 319: 158–158.

Yentsch, S. C., 1984. Remote assessment of ocean color for interpretation of satellite visible imagery: a review. The Quarterly Review of Biology 59: 348.

Yoder, J. A., S. E. Schollaert & J. E. O'Reilly, 2002. Climatological phytoplankton chlorophyll and sea surface temperature patterns in continental shelf and slope waters off the northeast US coast. Limnology and Oceanography 47: 672–682.

Yu, H., Q. M. Cai & J. L. Wu, 2003. Study on characteristic of the absorption and scattering coefficients of Lake Taihu waters. Advances in Water Science 14: 46–49 (in Chinese).

Yuan, D. & C. D. Elvidge, 1996. Comparison of relative radiometric normalization techniques. ISPRS Journal of Photogrammetry and Remote Sensing 51: 117–126.

Zhang, Y. L., M. L. Liu, B. Q. Qin, H. J. van der Woerd, J. S. Li & Y. L. Li, 2009. Modeling remote-sensing reflectance and retrieving chlorophyll-*a* concentration in extremely turbid case-2 waters (Lake Taihu, China). IEEE Transactions on Geoscience and Remote Sensing 47: 1937–1948.

Zhu, G. W., 2008. Eutrophic status and causing factors for a large, shallow and subtropical Lake Taihu, China. Hupo Kexue 20: 21–26 (in Chinese).